

Timing and Origin of Gold Mineralization in the Blueberry Zone of the Scottie Gold Mine Project, Stikine Terrane, Northwestern British Columbia (NTS 104D/01)

A. Hutchison¹, Department of Geology, Saint Mary's University, Halifax, Nova Scotia and Mount Royal University, Calgary, Alberta, alex.hutchison@smu.ca

M. Stewart, Department of Geology, Mount Royal University, Calgary, Alberta

J. Hanley, Department of Geology, Saint Mary's University, Halifax, Nova Scotia

R.C. Stewart, Serac Exploration Ltd., Vancouver, British Columbia

Hutchison, A., Stewart, M., Hanley, J. and Stewart, R.C. (2023): Timing and origin of gold mineralization in the Blueberry zone of the Scottie Gold Mine project, Stikine terrane, northwestern British Columbia (NTS 104D/01); in Geoscience BC Summary of Activities 2022: Minerals, Geoscience BC, Report 2023-01, p. 13–24.

Introduction

The 'Golden Triangle' is a mineral district in northwestern British Columbia (BC) that encompasses gold and porphyry-copper deposits, epithermal polymetallic deposits and volcanogenic massive-sulphide (VMS) base- and precious-metal deposits. The Golden Triangle contains the Scottie Gold Mine project, which consists of over thirty mineralized zones located within the Iskut–Stewart–Kitsault belt of the Stikine terrane. The Scottie Gold Mine project comprises three main zones across approximately 4 km: the Blueberry zone, the Scottie Gold Mine zone and the Domino zone. The mineralization trend of the Blueberry zone has a north-south orientation and is juxtaposed against the easterly trend of the Scottie Gold Mine and Domino zones. The focus of this study is to determine the timing and origin of gold mineralization in the Blueberry zone of the Scottie Gold Mine project, with the larger objective of determining the relationship between the Blueberry mineralization trend and the Scottie Gold mine mineralization trend. This will be done by combining detailed field mapping and drillcore sampling with petrography, whole-rock and mineral chemical analyses, as well as microanalytical methods (e.g., fluid-inclusion systematics), to achieve several specific outcomes:

- describe the hostrock units, alteration assemblages and ore-zone mineralogy for the Blueberry zone
- determine which minerals are typically associated with gold
- establish a paragenesis for the Blueberry zone that will be integrated with the deformation history
- compare the timing and style of gold mineralization in the Blueberry zone with those in the Scottie Gold Mine and Domino zones

This research aims to improve ore-deposit models and revise exploration criteria for epithermal-porphyry gold deposits in northwestern BC.

Background

Regional Geology

The Cordilleran orogeny resulted in terrane accretion along the western margin of the North American craton beginning in the Early to Middle Jurassic (Colpron et al., 2015). The tectonic domains of the Cordilleran Orogen are, from inboard to outboard, the Intermontane terranes, the Insular terranes, the Arctic terranes as well as the Mesozoic and younger arc and accretionary terranes (Nelson and Colpron, 2007). The terranes of the Intermontane belt were the earliest to be accreted and consist predominantly of island-arc terranes that developed in the peri-Laurentian realm (Nelson and Colpron, 2007). The Stikine terrane is one of these Intermontane island-arc terranes and preserves evidence of island-arc magmatism, sedimentation and deformation from its initial development, in the Late Devonian to Late Triassic, through to terminal collision with the North American craton (Evenchick et al., 2010; Colpron et al., 2015; Milidragovic et al., 2016). The Stikine terrane is subdivided into four stratigraphic units that are all separated by unconformities: the Devonian–Permian Stikine assemblage, the Upper Triassic Stuhini Group, the Lower to Middle Jurassic Hazelton Group and the Upper Jurassic to Lower Cretaceous Bowser Lake Group (Figure 1; Nelson et al., 2013). The Stikine terrane contains the major precious- and base-metal deposits that together define the area known as the 'Golden Triangle.' The development of the mineral deposits in the Golden Triangle was most prominent between the Late Triassic to Middle Jurassic and deposit types include Cu±Au±Mo porphyry deposits, Au-Ag epithermal deposits and VMS deposits (e.g., Barresi et al., 2015; Cutts et al., 2015). The intrusions associated with these mineral deposits can be subdivided into three groups based on their

¹The lead author is a 2022 Geoscience BC Scholarship recipient.

This publication is also available, free of charge, as colour digital files in Adobe Acrobat® PDF format from the Geoscience BC website: <http://geosciencebc.com/updates/summary-of-activities/>.

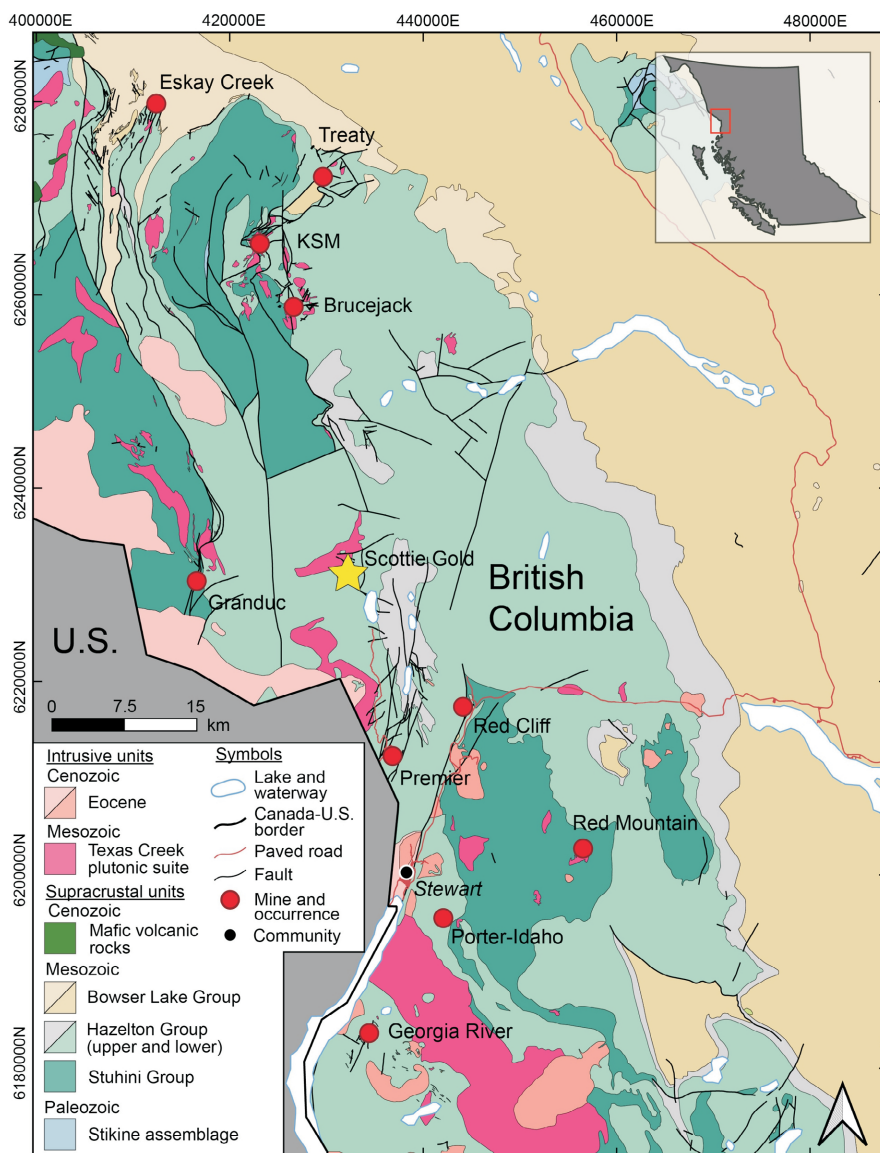


Figure 1. Regional geology of the Iskut–Stewart–Kitsault mineral belt (modified after Cui et al., 2017); the yellow star indicates the location of the Scottie Gold Mine project. All co-ordinates are in UTM Zone 9, NAD 83.

ages: late Triassic (ca. 222–210 Ma), terminal Triassic (205–201 Ma) and early Jurassic (197–190 Ma; Barresi et al., 2015). The Stuhini and Hazelton groups are associated both spatially and temporally with these mineralizing intrusions (Barresi et al., 2015).

The Hazelton Group is one of the major mineralization-hosting sequences within the Golden Triangle and comprises the study area (Figure 1). It unconformably overlies the Upper Triassic Stuhini Group, which consists of submarine mafic to intermediate volcanic rocks and epiclastic rocks, including shale, siltstone and limestone units; it is itself unconformably overlain by the sedimentary rocks of the Upper Jurassic to Lower Cretaceous Bowser Lake Group (Nelson and Kyba, 2014; Nelson et al., 2018). The Hazelton Group hosts substantial amounts of metallic ore

(Au, Ag, Cu) and is comagmatic and coeval with several plutonic suites, including the latest Triassic Tatogga suite and the Early Jurassic Texas Creek and Brucejack Lake suites (Evenchick et al., 2010; Voordouw and Branson, 2021; Nelson et al., 2022). The Hazelton Group is subdivided into upper and lower sequences, and the units within each of these sequences vary from north to south (Nelson et al., 2018). In the Unuk River–lower Iskut River–Stewart area, the lower Hazelton Group consists of the basal siliciclastic Jack Formation and the Snippaker unit, as well as the Betty Creek Formation (Nelson et al., 2018). The Betty Creek Formation is predominantly andesite with lesser occurrences of felsic pyroclastic rocks and their epiclastic products; it also contains the Unuk River andesite unit, the Johnny Mountain dacite unit and the Brucejack

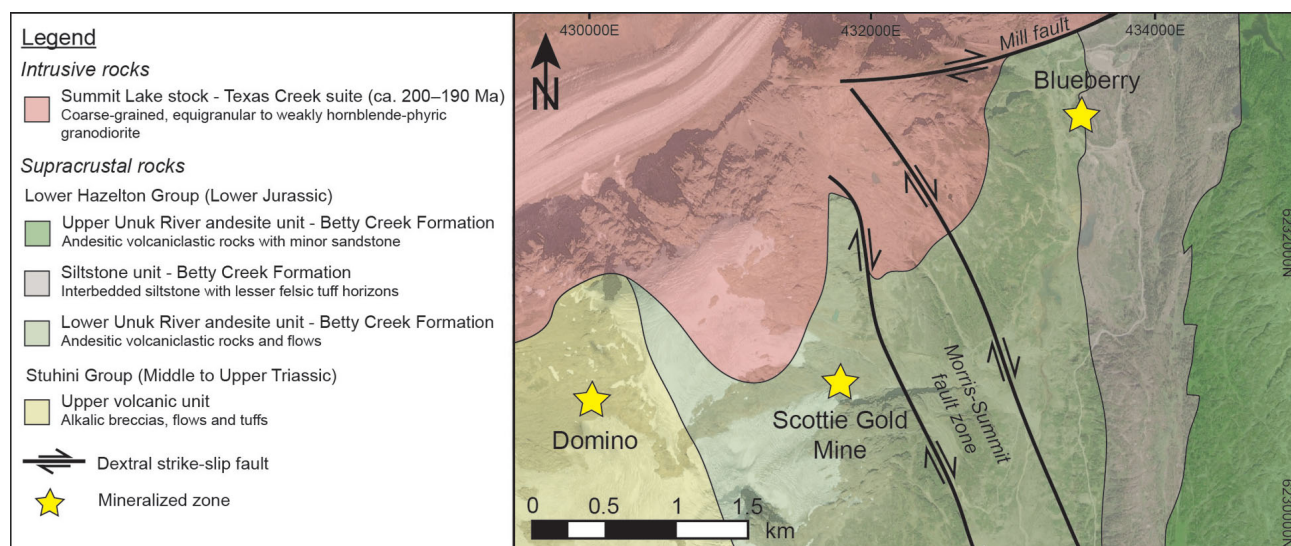


Figure 2. Geology of the Scottie Gold Mine project area. All co-ordinates are in UTM Zone 9, NAD 83.

Lake felsic unit (Nelson et al., 2018). The Unuk River andesite unit has been dated at ca. 197 Ma using U-Pb zircon geochronology (Nelson et al., 2018). In the study area, the upper Hazelton Group contains the Spatsizi, Quock and Mount Dilworth formations (Nelson et al., 2018).

Deposit Geology

The Scottie Gold Mine project is located approximately 30–35 km north of Stewart, BC, and comprises the Blueberry, Scottie Gold Mine and Domino zones (Figure 2). The Scottie Gold Mine project area is underlain by rocks of the Stuhini and Hazelton groups and intruded by Early Jurassic Texas Creek plutons (Figure 1; Stanley et al., 2022). The hostrocks to the Domino zone are alkalic volcanic flows, breccia and tuff of the Stuhini Group (Stanley et al., 2022); the hostrocks to the Scottie Gold Mine zone are volcanoclastic rocks and flows of the lower Unuk River andesite, which belongs to the Betty Creek Formation (Figure 2; Stanley et al., 2022). The Blueberry zone is interpreted to be located at the contact between the lower Unuk River andesite and the siltstone unit, which also belongs to the Betty Creek Formation (Figure 2; Stanley et al., 2022). This siltstone unit will herein be referred to as the ‘Betty Creek siltstone unit’. The contact between the lower Unuk River andesite and the Betty Creek siltstone unit defines a steeply dipping, northerly mineralization trend, whereas mineralization at the Domino and Scottie Gold Mine zones defines an easterly trend (Voordouw and Branson, 2021). The contact at the Blueberry zone exhibits strong and pervasive chlorite-pyrite-carbonate alteration and this alteration zone is approximately 15 to 30 m thick (Voordouw and Branson, 2021). Drilling and surficial mapping support the presence of east-northeast-striking mineralized-vein structures that intersect the Blueberry zone contact and may be indicative of high-grade gold mineralization. The highest concentra-

tions of gold mineralization have been documented along north-plunging ore shoots that occur at the intersection between the contact and these crosscutting veins (e.g., Blueberry vein; Voordouw and Branson, 2021). The Blueberry zone is also separated from the Scottie Gold Mine and Domino zones by the Morris-Summit fault zone (Figure 2; Stanley et al., 2022); however, the relationship between this fault zone and mineralization is currently unknown.

Methodology

During the 2021 field season, three 2020 drillholes were re-logged and mapping of the surficial materials was completed at the Blueberry zone, with the goal of documenting changes in lithology, alteration and mineralization (including hydrothermal vein types). Samples were initially selected to ensure representative coverage of all vein and alteration styles. Using available assay data, additional samples were selected using the following criteria: zones with high sulphide content and high gold concentrations, zones with high sulphide content and low gold concentrations, and zones with low sulphide content and high gold concentrations. These additional samples were collected to examine the relationship between gold and sulphide mineralization, and to determine why gold concentrations do not always correlate with sulphide zones. Two of three drillholes were selected from the northern half of the property (SR20–48 and SR20–55; Mumford, 2021) and the third drillhole was selected from the southern half of the property (SR20–45; Mumford, 2021). Drillcore samples, outcrop samples and pulps were sent to ALS-Geochemistry (Terrace, BC) for processing and analysis to evaluate Au, Ag, Co, Cu, Pb and Zn tenors, but also to generate a geochemical database for study purposes. Pulp samples are previously sampled, pulverized and assayed core samples for which a new aliquot was re-assayed. Drillcore and outcrop

samples underwent the following sample-preparation and analytical procedures:

- determination of Au by fire assay of 30 g samples (for low-range determination between 0.005 to 10 ppm)
- determination of Au by fire assay, with gravimetric finish of 30 g samples (for high-range determination between 0.05 to 10 000 ppm)
- four-acid digestion, with inductively coupled plasma–mass spectrometry (ICP-MS) finish of 0.25 g samples
- four-acid digestion, with overlimit methods using 0.4 g samples (ALS, 2022).

Pulps underwent the following procedures:

- determination of Au by fire assay of 30 g sample, with a range between 0.005 and 10 ppm
- four-acid digestion, with ICP-MS finish of 0.25 g sample (ALS, 2022).

Thirty-six thin sections were produced at Vancouver Petrographics Ltd. (Vancouver, BC) from core (23 sections) and outcrop (13 sections) samples for petrographic work and to facilitate ongoing microanalysis at Saint Mary’s University in Halifax, Nova Scotia. Transmitted- and reflected-light microscopy, scanning electron microscopy (SEM) and micro-X-ray–fluorescence (μ XRF) spectrometry enabled detailed petrography and semiquantitative chemical analysis of minerals. Transmitted- and reflected-light microscopy was performed using an Olympus BX51 microscope at Saint Mary’s University; photomicrographs were taken using a microscope-mounted, high-resolution digital camera.

Scanning Electron Microscope (SEM)

Backscattered-electron (BSE) imaging and semiquantitative energy-dispersive–X-ray spectroscopy (EDS) analysis of sulphides, silicates and other associated accessory phases (including gold carriers) were performed at Saint Mary’s University using a TESCAN MIRA3 LMU field emission–scanning electron microscope (FE-SEM) equipped with a X-Max 80 mm² large area silicon drift detector (SDD) energy-dispersive–X-ray spectrometer manufactured by Oxford Instrument. The electron-beam spot size was ~10 nm in diameter and the accelerating voltage used was 20 kV, together with a beam current of ~0.3 nA. The INCA software published by ETAS was used for data reduction and EDS-spectrum acquisition. This technique was used on thin sections created from both field and core samples to better understand general mineralogy as well as the timing of gold mineralization within the overall mineral-assembly paragenesis.

Micro-X-Ray Fluorescence

False-colour element-abundance maps were produced using a Bruker M4 Tornado Plus μ XRF spectrometer at Saint Mary’s University to map major-, minor- and trace-element

distribution on the surface of thin-section offcuts. Analyses were conducted under vacuum using a Rh X-ray source operated at an accelerating voltage of 50 kV and beam current of 600 μ A, focused to a 20 μ m diameter excitation spot size. Data was processed using software developed for the Bruker M4 Tornado scanner. The detector throughput was 275 000 cps and calibration was carried out on Zr. Pixels in element-abundance maps are spaced at 40 to 80 μ m and the count time per pixel was 30 ms.

Results

Surficial Mapping

Surficial mapping at the Blueberry zone during the 2021 field season improved spatial definition of the contact between the lower Unuk River andesite unit to the west and the Betty Creek siltstone unit to the east; the results of this mapping exercise are summarized in Figure 3. Within the map area, the lower Unuk River andesite unit is characterized by medium green-grey andesitic tuff with ash- to lapilli-sized grains. The Betty Creek siltstone unit is dominantly dark green, fine grained and bedded, but along-strike lithofacies variations are observed. In the northernmost section of the map area, this unit is dominated by argillite, which is very fine grained, dark grey to black and overprinted by intense silicification. In the southern portion of the map area, the siltstone is interbedded with cream-coloured felsic pyroclastic beds. The contact between the andesite and the siltstone appears to be gradational; however, it is completely overprinted by alteration. The zone of intense alteration along the contact has been broken out as a separate unit on the map because it obscures the exact location and nature of the contact (Figures 3, 4a–c). Figure 4a shows an outcrop from the northern extent of the map area; where the contact zone is crosscut by a medium green-grey, altered and weakly mineralized porphyritic lamprophyre dike with euhedral hornblende laths. An example of a southern outcrop and hand sample within the contact zone is shown in Figure 4b and c, respectively. The contact zone is also crosscut at a high angle by several interpreted faults. These faults are not exposed at surface, but the units are clearly offset and the faults have been intersected in drillcore.

Alteration

Alteration at the Blueberry zone is localized at the contact between the lower Unuk River andesite unit and the Betty Creek siltstone unit. The alteration is most intense at the contact and decreases in intensity moving outward from the contact zone. The alteration styles observed within the contact zone are the following:

- weak to moderate carbonate and silica alteration with a patchy to pervasive distribution (Figure 5a)

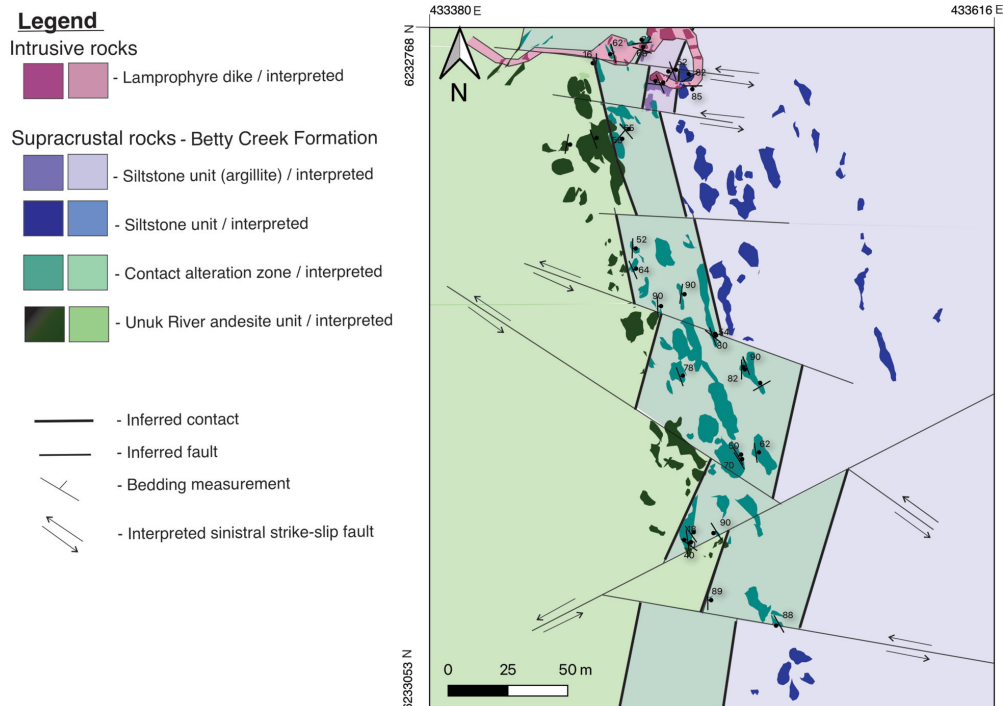


Figure 3. Geology of the Blueberry zone of the Scottie Gold Mine project. All co-ordinates are in UTM Zone 9, NAD 83.

- weak to moderate chlorite alteration that is dominantly patchy (Figure 5b), but also locally occurs as pervasive or fracture-controlled alteration, as vein selvages or along bedding planes
- moderate to strong sericite alteration that is typically patchy and less frequently pervasive (Figure 5a–c)
- weak epidote alteration that is patchy (Figure 5c) or within vein selvages

Sericite alteration is typically most closely associated with sulphide mineralization; however, this is a preliminary observation and the relative timing of the various alteration styles and their relationship to sulphide and gold mineralization are currently under investigation.

Sulphide Mineralization

Sulphide mineralization in the Blueberry zone occurs both within the zone of intense alteration along the andesite–siltstone contact (the ‘contact zone’; Figure 3) and along a series of faults that crosscut the contact at a high angle. These mineralization styles are described below.

Contact Zone

Mineralization in the contact zone is disseminated, within veins and along vein selvages. Based on fieldwork, drill-core observations and transmitted- and reflected-light microscopy, the dominant base-metal sulphide minerals present within the contact zone are, in descending order of abundance, pyrrhotite, pyrite, sphalerite, chalcopyrite, arsenopyrite, galena and molybdenite. The average modal

sulphide abundance across the entire contact zone is approximately 2–4 vol %; however, mineralized veins contain 10–50 vol % sulphides. Pyrrhotite and pyrite (with lesser chalcopyrite) occur disseminated within the groundmass, within massive sulphide veins (~1–3 cm wide), along the margins of quartz-carbonate veins, along bedding planes and within pyrite-dominated stringers. Pyrrhotite is the most abundant sulphide mineral and is present as anhedral masses that tend to be mottled, often surrounding other sulphide minerals (pyrite, chalcopyrite, arsenopyrite; Figure 6a–c). Pyrite is present as subhedral to euhedral crystals (<0.5–6 mm) in two forms: mottled (Figure 6a–c) and inclusion-free. Chalcopyrite is spatially associated with pyrite but is less abundant. It occurs as anhedral patches and is often disseminated around pyrite crystals or within fractures cutting pyrite crystals (Figure 6b). Where arsenopyrite is present, it tends to be concentrated in patches of euhedral to subhedral crystals up to ~3 mm wide (Figure 6a, c) and, like pyrite, it occurs as mottled and inclusion-free varieties. Inclusion-free arsenopyrite defines a linear fabric within the groundmass, separate from other sulphide minerals (Figure 6a), whereas mottled arsenopyrite is typically surrounded by pyrrhotite. The two arsenopyrite varieties also vary chemically, with inclusion-free arsenopyrite being enriched in both Sb and Co, whereas mottled arsenopyrite is enriched only in Co (1.37–3.53 wt % Sb and 2.99–3.69 wt % Co, and 4.89–29.15 wt % Co, respectively, in mottled arsenopyrite). Sphalerite is most commonly present within extensional quartz-

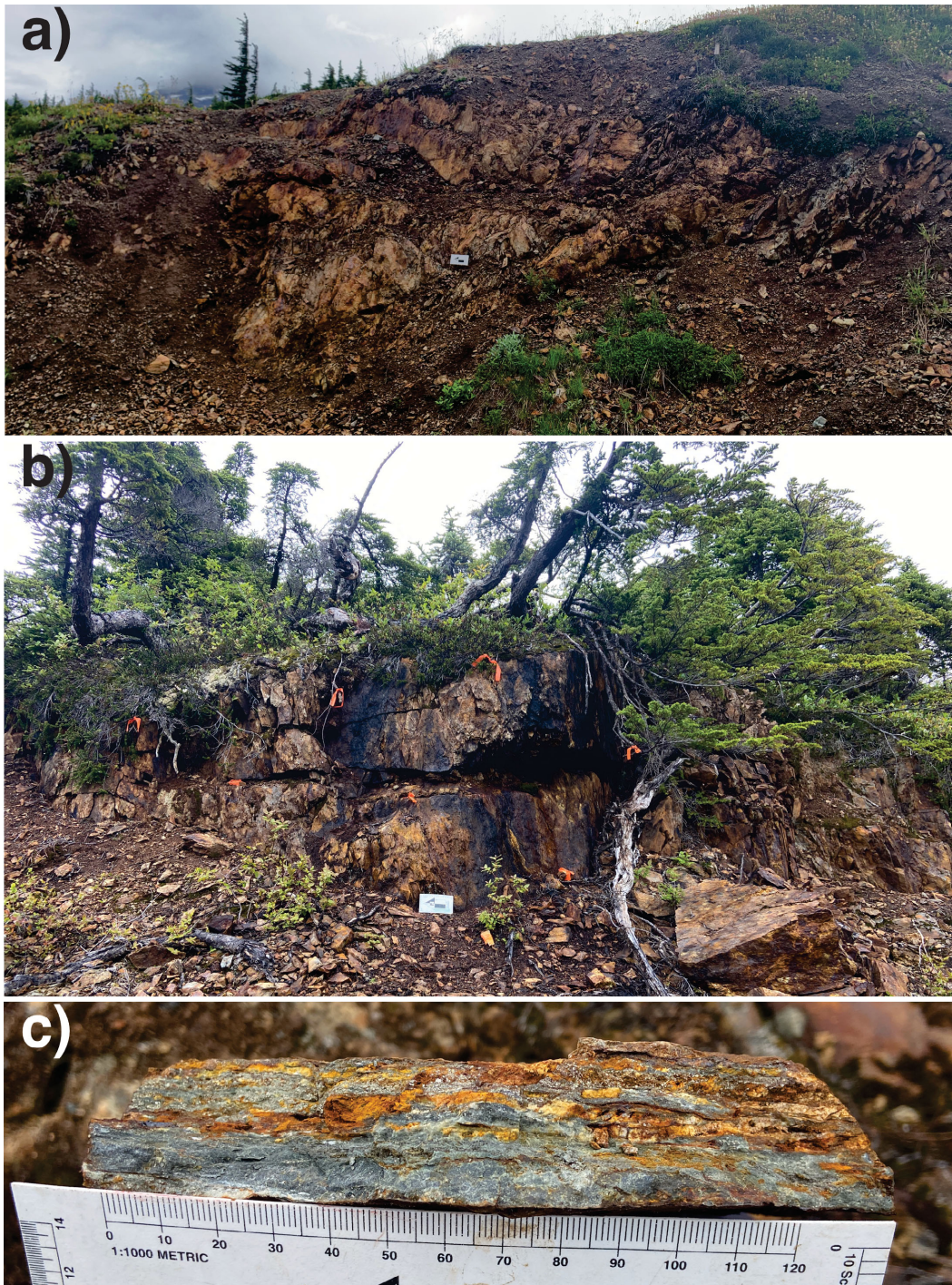


Figure 4. Field photographs showing outcrops within the gossanous central alteration zone of the Blueberry zone: **a)** northern outcrop; **b)** southern outcrop; **c)** hand sample from southern outcrop (12 cm scale card used for reference).

carbonate veins and larger extensional quartz-carbonate veins (<1–3 cm wide) also contain trace amounts of galena and molybdenite. Sphalerite occurs as inclusions within pyrrhotite and filling fractures within Co-rich arsenopyrite. Molybdenite typically occurs as isolated subhedral crystals ranging from 10 to 40 μm in width and its relationship to other sulphide minerals is unclear. The exception is galena

that often occurs as inclusions within molybdenite. It appears that sulphides are less abundant extending into the sedimentary side of the contact relative to the andesite side, but mineralization is uniformly distributed within the main alteration zone. Arsenopyrite is an exception and tends to be concentrated dominantly in the southern half of the Blueberry zone.

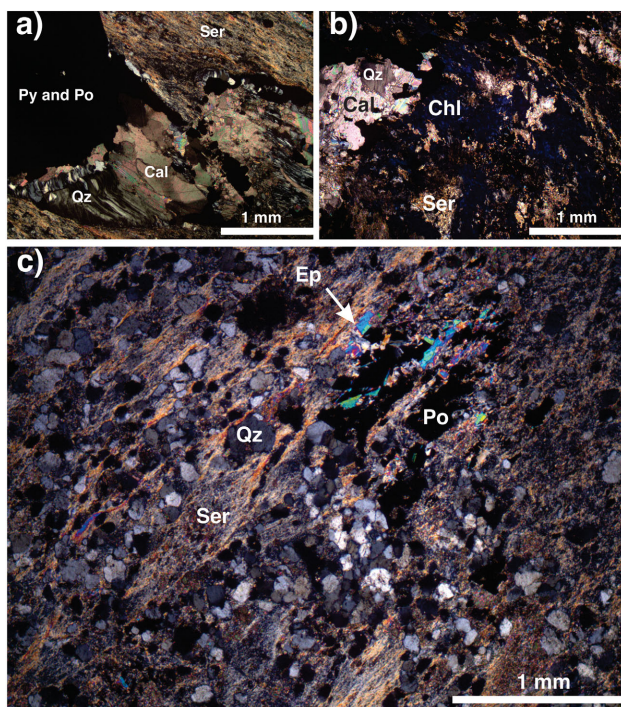


Figure 5. Photomicrographs taken in cross-polarized light of the dominant alteration minerals at the contact zone between the lower Unuk River andesite unit and the Betty Creek siltstone unit: **a)** patchy calcite (Cal) and kink-banded quartz (Qz) spatially associated with sulphide minerals and presence of very fine-grained sericite (Ser) in the groundmass; **b)** patchy carbonate and quartz crystals within a groundmass of fine- to very fine-grained chlorite (Chl) and sericite; **c)** rounded, subhedral quartz crystals crosscut by very fine-grained sericite and patchy, medium-grained epidote (Ep) crystals spatially associated with pyrrhotite (Po). Abbreviation: Py, pyrite.

Both mineralized and barren veins are observed within the contact zone and these veins can be classified into four main types:

- quartz-dominated veins consisting of fine- to medium-grained intergrown quartz crystals
- type-1 calcite-dominated veins consisting of fine- to very fine-grained calcite and defined by the absence of sulphide minerals
- type-2 calcite-dominated veins consisting of very fine-grained calcite and defined by the presence of sulphide minerals along the centre axes of the veins, with alteration minerals like epidote and accessory minerals like apatite
- extensional quartz-calcite veins containing some sulphides

The dominant sulphides in type-2 calcite veins are pyrrhotite and pyrite, and the average modal abundance of sulphides in these veins is ~30–50%. The dominant sulphides in the extensional veins are sphalerite, molybdenite and galena, and the modal abundance of sulphides in these veins is ~10–15%.

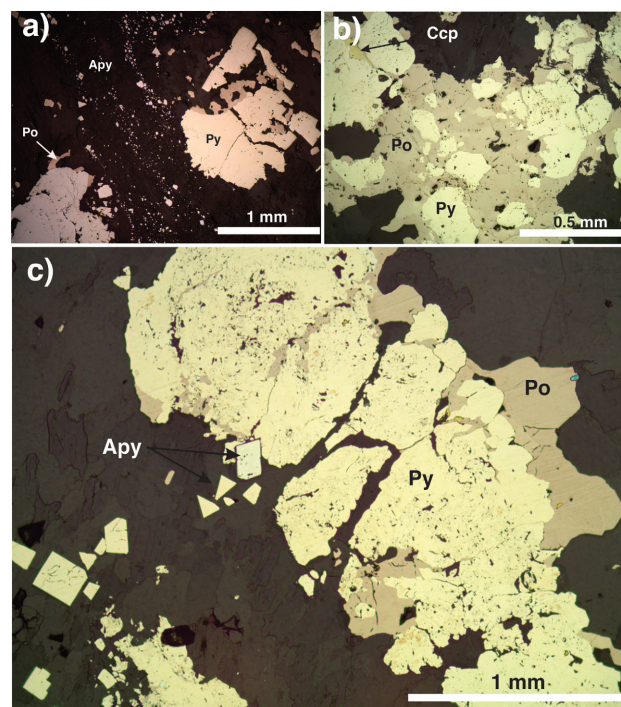


Figure 6. Sulphide-mineral relationships of the Blueberry zone shown in reflected light: **a)** mottled pyrite (Py) surrounded by pyrrhotite (Po), with euhedral to subhedral arsenopyrite (Apy) crystals defining a linear fabric; **b)** mottled pyrite surrounded by chalcopyrite (Ccp) and pyrrhotite; **c)** mottled pyrite surrounded by pyrrhotite, with an early arsenopyrite crystal near the centre.

Mineralized Crosscutting Structures

Several faults are interpreted as crosscutting the contact zone at a high angle (Figure 3) and drill results to date indicate that at least three of these structures host mineralization, which ranges from disseminated to semi-massive, with pyrrhotite, pyrite and sphalerite as the dominant sulphide minerals. These structures are interpreted to be significant for the distribution and localization of mineralization along the contact zone. However, additional work is required to correlate the surface trace of the faults with the mineralized structures intersected in drillcore and to determine the relationship between mineralization in the contact zone and the crosscutting faults. Additional drillcore samples were collected from these structures in 2022 and analyses of these samples are currently underway.

Gold Occurrences

The highest gold concentrations returned during the 2020 drilling program were intersected within the altered contact zone of the northernmost drillholes of the Blueberry Zone (SR20–48 and SR20–55). The highest gold-bearing intervals in SR20–48 are at downhole depths of 18.07–19.08 m (82.1 g/t) and 68.62–70.35 m (69.8 g/t; Mumford, 2021). The highest gold-bearing interval in SR20-55 is at a downhole depth of 78.97–79.75 m (47.9 g/t; Mumford, 2020). In both intervals, gold is spatially associated with sulphide

minerals, including pyrite, arsenopyrite, pyrrhotite and molybdenite. Where it is associated with pyrite, gold occurs as 5–10 µm diameter inclusions (Figure 7a, b) within euhedral to subhedral mottled pyrite crystals. Gold associated with arsenopyrite also occurs as inclusions; arsenopyrite crystals containing gold are typically subhedral, mottled and Co-rich (Figure 7c). Where gold occurs with molybdenite, they exhibit a close spatial relationship, with observed intergrowth textures between gold and molybdenite (Figure 7d).

Discussion

A preliminary paragenesis for alteration, veining and associated mineralization on a time scale spanning magmatic to late magmatic-hydrothermal events is being developed.

Mineralization

Key textures constrain overall sulphide-mineral paragenesis. Pyrite, pyrrhotite (Figure 7a–c) and chalcopyrite (Figure 6b) tend to be spatially associated with one another, therefore broadly coeval. As stated earlier, pyrite is present as subhedral to euhedral crystals in two forms: mottled and inclusion free. Dissolution and reprecipitation of pyrite

likely resulted in the mottled appearance, but later conditions allowed pyrite to grow and maintain a subhedral shape. This indicates potentially two generations of pyrite, whereby the mottled form (Figure 7b) is an earlier generation in comparison to the inclusion-free form (Figure 7a). Pyrite grains range from <0.5 to 2 mm in width. Textural relationships between the mottled-type pyrite, pyrrhotite, chalcopyrite and mottled arsenopyrite are shown in Figures 6b (chalcopyrite) and 7a–c. This pyrite likely precipitated first in the sulphide-mineral sequence, whereas chalcopyrite and, later, pyrrhotite infilled the space around the earlier subhedral pyrite owing to the general subhedral to euhedral nature of pyrite. Chalcopyrite is less abundant relative to pyrite; it forms as anhedral patches and is often disseminated in available space near pyrite crystals. Like pyrite, arsenopyrite is also present in two forms: mottled and inclusion free. Unmottled or inclusion-free arsenopyrite is euhedral and occurs as lineations away from other sulphide minerals within groundmass. The timing relationship between the linear wash of un-mottled arsenopyrite (Figure 6a) in relation to pyrrhotite and pyrite in these images is not evident, though the single mottled crystal slightly to the left of centre in Figure 6c appears to be early in relation to pyrite and pyrrhotite. The un-mottled arsenopyrite tends to

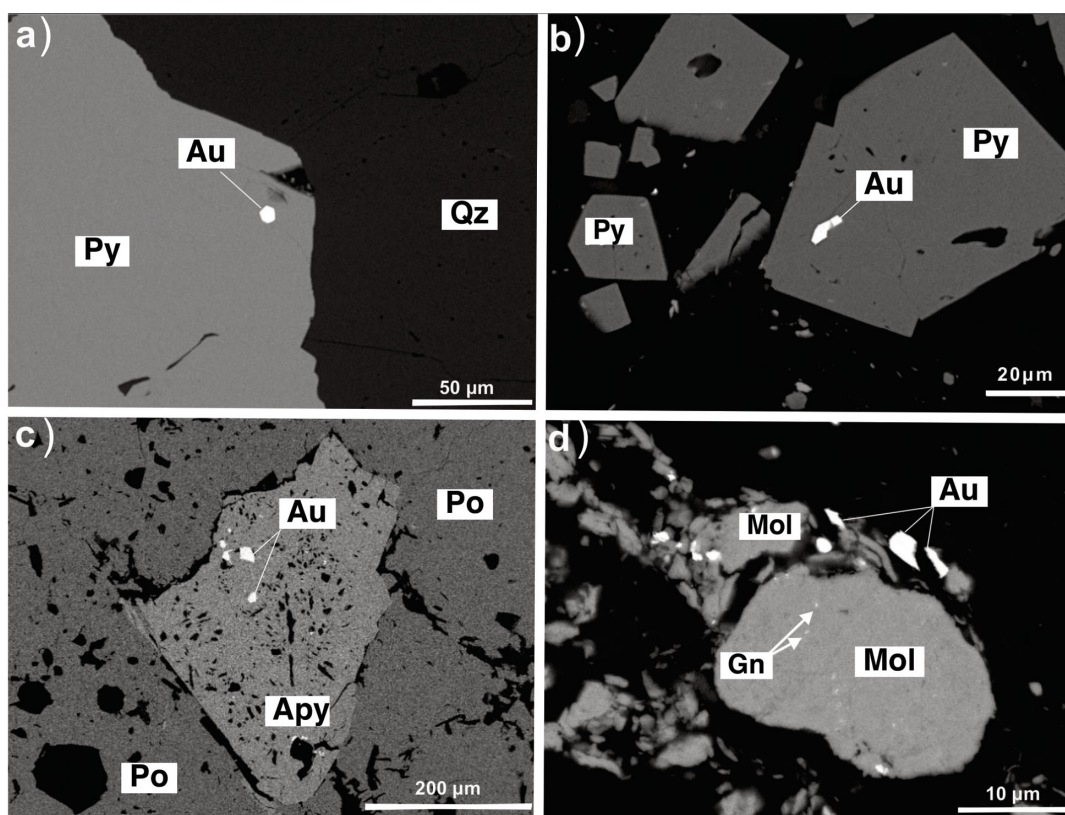


Figure 7. Backscattered-electron images of gold mineralization and associated sulphide minerals in the Blueberry zone: **a)** gold (Au) grain within an inclusion-free pyrite (Py) crystal; **b)** euhedral to subhedral pyrite crystals with some mottling and gold occupying an open space in a pyrite crystal; **c)** heavily mottled Co-rich arsenopyrite (Apy) crystal surrounded by mottled pyrrhotite (Po) and gold occupying open spaces in the arsenopyrite crystal; **d)** small gold grains (<1–3 µm) spatially associated with larger (up to 20 µm) crystals of molybdenite (Mol), as well as flecks of galena (Gn) visible within the molybdenite crystals. Abbreviation: Qz, quartz.

be a combination of both the Sb- and Co-enriched varieties. Mottled arsenopyrite is enriched only in Co and surrounded by pyrrhotite, although the open spaces of Co-enriched arsenopyrite contain gold inclusions (Figure 7c). Pyrrhotite is most abundant relative to the other sulphide minerals and is present as anhedral crystals. It is commonly found surrounding other sulphide minerals (pyrite, chalcopyrite and arsenopyrite), indicating late precipitation relative to the other sulphides.

Sphalerite inclusions occur in pyrrhotite, indicating that it postdates the precipitation of pyrrhotite; also, sphalerite commonly infills cracks in Co-rich arsenopyrite associated with pyrrhotite (not shown here). Galena is included within molybdenite, therefore likely coprecipitating with it (Figure 7d). Lastly, whereas intergrowths of gold and molybdenite are indicative of coprecipitation, no other obvious crosscutting relationships with other sulphides are observed for molybdenite.

Alteration

With respect to alteration, petrographic work suggests epidote alteration, carbonatization, silicification and chloritization all occurred during the magmatic stage. In addition to quartz associated with veining at the contact alteration zone, there is evidence of silica flooding throughout the groundmass, which is crosscut by later chlorite alteration. There is also evidence of chlorite crosscut by silica, indicating that silica may have been precipitated broadly coevally with chlorite in the groundmass. Sericite is introduced coevally with chlorite and toward the latter end of silica precipitation. Figure 5c shows coarse epidote crystals (relative to sericite grain size in the groundmass) precipitated near sulphide minerals (e.g., pyrrhotite). The subhedral shape of the pyrrhotite crystals sharing crystal boundaries with epidote suggests that epidote and pyrrhotite precipitated at a similar time. Sericite may have also been broadly coeval to late in terms of pyrrhotite precipitation, as crystal boundaries appear to be torn off the crystal in places but also growing together in others. Sericite and epidote appear to most commonly coprecipitate with sulphide mineralization. Sericitization occurs late in the system (magmatic to late magmatic/hydrothermal stage) and, in terms of alteration minerals, occurs nearest in time to the late precipitation of sulphide minerals. Sericite appears to overprint all other alteration minerals but indicates coeval precipitation with pyrrhotite. The exact relationship is unclear.

Vein and Structural Styles

It is important to constrain the relationship between the crosscutting structures and the contact zone. In particular, if the abundance of sulphides, sulphide mineralogy and associated gold content vary along the contact zone, understanding the role that crosscutting veins played in the development of these variations in the Blueberry zone would be

beneficial to the deposit model. It would be useful to understand which structures transported the mineralizing fluid(s) and the timing of these events relative to one another; this information could then be paired with the microscopic evidence of these veining events (in addition to macroscopic evidence). In further developing the time scale described above, the following veining events are recognized:

- early quartz-dominated veining associated with the magmatic stage, consisting of fine- to medium-grained intergrown quartz crystals
- type-1 calcite-dominated veins, defined by a lack of sulphide minerals and the presence of fine- to very fine-grained calcite, that crosscut and, therefore, postdate the early quartz veins but are also still considered to be within the magmatic stage
- type-2 calcite-dominated veins containing sulphide minerals and considered to be associated with the transition from the magmatic to later magmatic-hydrothermal stage as there is a sulphide component, as well as alteration minerals like epidote and apatite (type-2 calcite veins)

Gold Occurrences

Along the mineralized contact zone, gold is associated with pyrite, pyrrhotite, arsenopyrite and molybdenite. Pyrite, pyrrhotite and arsenopyrite typically exhibit a close spatial relationship (occasionally with sphalerite) in the presence of gold, whereas sphalerite, galena and molybdenite commonly occur together within extensional, gold-bearing quartz-carbonate veins. This indicates that gold occurs in two distinct textural settings (and, therefore, distinct timings): disseminated with pyrite, pyrrhotite and arsenopyrite in veins and groundmass; and with disseminated and patchy sphalerite and molybdenite in quartz-carbonate veins. These two textural relationships involving gold may indicate changing conditions within a single hydrothermal mineralizing event (e.g., fluid temperature, pH, gold complexing) or that more than one gold-mineralizing event occurred. Gold was deposited during a magmatic-hydrothermal mineralizing event and later remobilized. The timing of gold mineralization in relation to other sulphide minerals is complex. Gold occurs within the open space of euhedral to subhedral pyrite crystals, indicating possible late precipitation of gold relative to pyrite. Additionally, gold is intergrown with subhedral to anhedral pyrite crystals, suggesting that it is coeval with this type of pyrite. This could mean the timing of pyrite and gold formation could be close and/or overlap. Pyrrhotite is present following the precipitation of arsenopyrite, but the timing between pyrrhotite and gold precipitation is unknown. The mottled texture of the pyrrhotite could be a result of alteration (Figures 6b, c, 7c).

Molybdenite and Arsenopyrite

Molybdenum mineralization along the western margin of the Stikine terrane precipitated during two distinct time periods: in the Lower Jurassic (Febbo et al., 2015), hosted within Au-Cu-Ag-Mo porphyry deposits associated with the Texas Creek plutonic suite; and in the early Eocene to Oligocene (Nelson and Colpron, 2007), hosted within Cu-Au-Mo- and Mo-porphyry deposits associated with intrusions of the mid-Cretaceous to mid-Eocene Coast Plutonic Complex or with small, Oligocene granitic intrusions. Given these disparate ages and a lack of textural clarity as to which generation of gold comes first in the overall deposit paragenesis, it is unclear whether gold associated with molybdenite represents early- or late-stage mineralization. This will be resolved through Re-Os radiometric dating of molybdenite. Additionally, gold is observed in open-space fillings associated with arsenopyrite crystals (Figure 7c), suggesting that gold precipitation postdates Co-rich arsenopyrite. A Re-Os age for arsenopyrite would thus provide a maximum age for gold precipitation. Given that gold may postdate arsenopyrite and be coeval with molybdenite, combined Re-Os radiometric dating of molybdenite and arsenopyrite together could tightly constrain the age of gold mineralization.

Co-Rich Arsenopyrite Versus Sb-Rich Arsenopyrite

Understanding the genetic relationship between gold and the different forms of arsenopyrite (i.e., Co- and Sb-rich) is potentially important to understanding the nature of gold mineralization at the Blueberry zone. Although Co- and Sb-enriched arsenopyrite occur together, they also occur isolated from one another. Notably, where Sb is present in arsenopyrite, gold is not. However, Co-enriched arsenopyrite also occurs with Sb-enriched arsenopyrite, both in the unmottled, euhedral form and with crystals showing alignment within the groundmass. In contrast, the mottled, subhedral Co-rich form of arsenopyrite contains gold in open-space fillings. Observations support that gold precipitation may have been more favourable under Sb-absent conditions, or when conditions were not suitable for Sb precipitation in pyrite.

Summary and Conclusions

The Blueberry zone is one of three main zones within the Scottie Gold Mine project. Locally, the host lithological units are the lower Unuk River andesite unit in the west and the Betty Creek siltstone unit in the east; the host units are separated by a north-trending contact. Based on field and drillcore observations, the contact between the two units appears to be gradational. Whether this is the case, or that the contact has been obscured by alteration and/or faulting remains unresolved. It is likely that this central alteration zone acted as a conduit for mineralizing fluids. In addition to mineralization at the contact, mineralization in the Blue-

berry zone also occurs along faults that cut the contact at a high angle. The relationship between mineralization in the contact zone and in the crosscutting faults is unclear and should be resolved. Samples were collected from outcrop and drillcore (from both the contact zone and the crosscutting structures) to petrographically characterize host rock lithology, the main alteration and vein styles, and the nature of gold mineralization, as well as to provide additional samples for assay. All work completed to date has been related to the contact zone and future work will incorporate data from the mineralized crosscutting structures, enabling a detailed description of mineralization at the Blueberry zone to be constructed.

In conclusion, the dominant alteration styles identified in the contact zone are predominantly weak to moderate carbonate alteration and silicification, weak to moderate chlorite alteration distributed in a variety of ways (patchy, disseminated, fracture-controlled, within vein selvages and along bedding planes), moderate to strong sericitization and weak epidote alteration. The sulphide minerals at the contact zone are, in order of decreasing abundance, pyrrhotite, pyrite, sphalerite, chalcopyrite, arsenopyrite, galena and molybdenite. Both Co-rich and Sb-rich arsenopyrite have been observed in samples from the contact zone and gold exhibits a stronger relationship with Co-rich arsenopyrite than Sb-rich arsenopyrite. Gold likely precipitated in the late stages of the system given the nature of gold as inclusions in the open spaces of arsenopyrite and pyrite. A key aspect of the mineralization to consider is whether gold has been remobilized or not, which will require further study.

Future Work

Additional samples were collected in 2022 along the mineralized structures that crosscut the contact zone. These samples will be used to investigate the influence of these structures on gold mineralization in the Blueberry zone. Gold concentrations vary significantly along the contact zone and it is important to understand if and how the crosscutting structures influence these variations in gold mineralization. Additionally, by gaining an understanding of the nature of each vein, it may be possible to identify the timing of the mineralizing fluid as well as the conduit(s) the fluids may have used. Given that magmatic to late magmatic-hydrothermal sulphide-rich calcite veining has been observed on a microscopic scale, a comparative study to see if these microscopic veining events coincide with the larger scale features responsible for gold mineralization would be useful. During a visit to the field in 2022, additional drillcore samples were also collected for fluid-inclusion work. Work planned for the remainder of this study includes

- detailed petrography of samples from the mineralized crosscutting structures to characterize the alteration and

mineralization for comparison with those in the contact zone;

- Re-Os radiometric dating of molybdenite and arsenopyrite associated with gold to determine the timing of gold mineralization;
- fluid-inclusion analysis of quartz from mineralized veins to characterize the mineralizing fluid(s); and
- laser-ablation inductively coupled plasma–mass spectrometry on individual pyrite grains to be used as a proxy for the chemical evolution of mineralization in the Blueberry zone.

The results of this detailed study on the Blueberry zone will be compared with the results of a parallel study on the Scottie Gold Mine zone to determine if these two zones belong to the same ore system and, if so, how the zones are related.

Acknowledgments

Funding for this project is provided by Scottie Resources Corp., Serac Exploration Ltd., Geoscience BC and the Natural Sciences and Engineering Research Council of Canada (NSERC) through the iMAGE-CREATE project. The authors particularly thank D. Guestrin of Serac Exploration Ltd. for his thoughtful and insightful comments, which greatly contributed to improving the manuscript.

References

- ALS (2022): Geochemistry, 2022 schedule of services and fees; ALS, 50 p., URL <<https://www.alsglobal.com/en/geochemistry/geochemistry-fee-schedules>> [October 2022].
- Barresi, T., Nelson, J.L., Dostal, J. and Friedman, R. (2015): Evolution of the Hazelton arc near Terrace, British Columbia: stratigraphic, geochronological, and geochemical constraints on a Late Triassic–Early Jurassic arc and Cu–Au porphyry belt; *Canadian Journal of Earth Sciences*, v. 52, no. 7, p. 466–494, URL <<https://doi.org/10.1139/cjes-2014-0155>>.
- Colpron, M., Crowley, J.L., Gehrels, G., Long, D.G.F., Murphy, D.C., Beranek, L. and Bickerton, L. (2015): Birth of the northern Cordilleran orogen, as recorded by detrital zircons in Jurassic synorogenic strata and regional exhumation in Yukon; *Lithosphere*, v. 7, no. 5, p. 541–562, URL <<https://doi.org/10.1130/L451.1>>.
- Cui, Y., Miller, D., Schiarizza, P. and Diakow, L.G. (2017): British Columbia digital geology; BC Ministry of Energy, Mines and Low Carbon Innovation, BC Geological Survey, Open File 2017-8, 9 p., URL <https://cmscontent.nrs.gov.bc.ca/geoscience/publicationcatalogue/OpenFile/BCGS_OF2017-08.pdf> [November 2022].
- Cutts, J.A., McNicoll, V.J., Zagorevski, A., Anderson, R.G. and Martin, K. (2015): U-Pb geochronology of the Hazelton Group in the McTagg anticlinorium, Iskut River area, northwestern British Columbia; *in Geological Fieldwork 2014*, BC Ministry of Energy, Mines and Low Carbon Innovation, BC Geological Survey, Paper 2015-1, p. 87–101, URL <https://cmscontent.nrs.gov.bc.ca/geoscience/publicationcatalogue/Paper/BCGS_P2015-01-05_Cutts.pdf> [November 2022].
- Evenchick, C.A., Poulton, T.P. and McNicoll, V.J. (2010): Nature and significance of the diachronous contact between the Hazelton and Bowser Lake groups (Jurassic), north-central British Columbia; *Bulletin of Canadian Petroleum Geology*, v. 58, no. 3, p. 235–267, URL <<https://doi.org/10.2113/gscpgbull.58.3.235>>.
- Febbo, G.E., Kennedy, L.A., Savell, M., Creaser, R.A. and Friedman, R.M. (2015): Geology of the Mitchell Au-Cu-Ag-Mo porphyry deposit, northwestern British Columbia, Canada; *in Geological Fieldwork 2014*, BC Ministry of Energy, Mines and Low Carbon Innovation, BC Geological Survey Paper 2015-1, p. 59–86, URL <https://cmscontent.nrs.gov.bc.ca/geoscience/PublicationCatalogue/Paper/BCGS_P2015-01-04_Febbo.pdf> [November 2022].
- Milidragovic, D., Chapman, J.B., Bichlmaier, S., Canil, D. and Zagorevski, A. (2016): H₂O-driven generation of picritic melts in the Middle to Late Triassic Stuhini arc of the Stikine terrane, British Columbia, Canada; *Earth and Planetary Science Letters*, v. 454, p. 65–77, URL <<https://doi.org/10.1016/j.epsl.2016.08.034>>.
- Mumford, T. (2020): Scottie Resources discovers new mineralization trend at Blueberry Zone, reports intercepts of 22.3 g/t over 6.1 m and 8.96 g/t over 13.7 m; Scottie Resources Corp., URL <<https://scottieresources.com/news/2020/thefirstresultsfromblueberry/>> [November 2022].
- Mumford, T. (2021): Scottie discovers new mineralization trend at Blueberry Zone, reports intercepts of 10.2 g/t gold over 3.21 m and 1.31 g/t over 22.13 m; Scottie Resources Corp., URL <<https://scottieresources.com/news/2021/scottie-discovers-new-mineralization-trend-at-blueberry-zone-reports-intercepts-of-10.2-g-t-gold-over-3.21-m-and-1.31-g-t-gold/>> [November 2022].
- Nelson, J. and Colpron, M. (2007): Tectonics and metallogeny of the British Columbia, Yukon and Alaskan Cordillera, 1.8 Ga to the present; *in Mineral Deposits of Canada: a Synthesis of Major Deposit Types, District Metallogeny, the Evolution of Geological Provinces, and Exploration Methods*, W.D. Goodfellow (ed.), Geological Association of Canada, Mineral Deposits Division, Special Publication, no. 5, p. 755–791.
- Nelson, J.A.L. and Kyba, J. (2014): Structural and stratigraphic control of porphyry and related mineralization in the Treaty Glacier–KSM–Brucejack–Stewart trend of western Stikinia; *in Geological Fieldwork 2013*, BC Ministry of Energy, Mines and Low Carbon Innovation, BC Geological Survey Paper 2014-1, p. 111–140, URL <https://cmscontent.nrs.gov.bc.ca/geoscience/publicationcatalogue/Paper/BCGS_P2014-01-07_Nelson.pdf> [November 2022].
- Nelson, J.A.L., Colpron, M. and Israel, S. (2013): The Cordillera of British Columbia, Yukon, and Alaska; *in Tectonics, Metallogeny, and Discovery: the North American Cordillera and Similar Accretionary Settings*, L. Colpron, T. Bissig, B.G. Rusk and J.F.H. Thompson (ed.), Society of Economic Geologists, Special Publications, v. 17, p. 53–109, URL <<https://doi.org/10.5382/sp.17.03>>.
- Nelson, J.A.L., van Straaten, B. and Friedman, R. (2022): Latest Triassic–early Jurassic Stikine–Yukon–Tanana terrane collision and the onset of accretion in the Canadian Cordillera: insights from Hazelton Group detrital zircon provenance and arc–back-arc configuration; *Geosphere*, v. 18, no. 2, p. 670–696, URL <<https://doi.org/10.1130/ges02444.1>>.
- Nelson, J., Waldron, J., van Straaten, B., Zagorevski, A. and Rees, C. (2018): Revised stratigraphy of the Hazelton Group in the

Iskut River region, northwestern British Columbia; *in* Geological Fieldwork 2017, BC Ministry of Energy, Mines and Low Carbon Innovation, BC Geological Survey Paper 2018-1, p. 15–38, URL <https://cmscontent.nrs.gov.bc.ca/geoscience/PublicationCatalogue/Paper/BCGS_P2018-01-02_Nelson.pdf> [November 2022].

Stanley, B., Nelson, J.L. and Friedman, R. (2022): LA-ICP-MS U-Pb data files, detrital zircon geochronology, and geochemistry of the Stuhini and Hazelton groups, Scottie gold mine area, northwestern British Columbia; BC Ministry of Energy, Mines and

Low Carbon Innovation, BC Geological Survey GeoFile 2022-08, 5 p., URL <https://cmscontent.nrs.gov.bc.ca/geoscience/PublicationCatalogue/GeoFile/BCGS_GF2022-08.pdf> [November 2022].

Voordouw, R. and Branson, T. (2021): Technical report on the Scottie Gold Mine Property, British Columbia, Canada; National Instrument 43-101 report prepared for Scottie Resources Corporation, 77 p., URL <https://scottieresources.com/site/assets/files/3826/scot_ni43-101report_20210507.pdf> [November 2022].